

FINAL REPORT

Bioaccumulation and trophic transfer of long-lived radionuclides in Arctic plankton

ONR Grant # N000149511229

1996

Nicholas S. Fisher

Professor

Marine Sciences Research Center
State University of New York
Stony Brook, NY 11794-5000

DISTRIBUTION STATEMENT E
Approved for public release
Distribution Unlimited

19980218 053

DTIC QUALITY INSPECTED 3

Bioaccumulation and trophic transfer of long-lived radionuclides in Arctic plankton

Principal Investigator: Nicholas S. Fisher

Address: Marine Sciences Research Center
State University of New York
Stony Brook, NY 11794-5000

E-mail: NFISHER@CCMAIL.SUNYSB.EDU

Telephone/Fax tel: (516) 632-8649
fax: (516) 632-8820

Narrative Documentation

A. Long-term goals

The long-term goal of this project is to understand how radionuclides are accumulated in Arctic marine food chains, focusing on the trophic transfer within lower levels of the food chain.

B. Objectives of this effort

The objectives of our research is to examine the bioaccumulation and trophic transfer of important radionuclides in important planktonic components of Arctic waters. This project has been assessing the extent to which select species of boreal copepod species bioconcentrate released radionuclides from water and from phytoplankton food. The rates and routes of uptake and depuration of isotopes in these animals was investigated.

C. Approach

In laboratory microcosm experiments employing radiotracer methodology, we have been examining the kinetics of uptake and release of Cs-137, Am-241, Eu-152, Fe-59, and Co-57 in marine phytoplankton (primarily diatoms) and calanoid copepods. This work has focused principally on the uptake of radionuclides from the dissolved phase for phytoplankton and uptake via trophic transfer in the zooplankton. The retention of the radionuclides in the organisms and their waste products (particularly fecal material and phytodetritus) has been quantified.

D. Accomplishments

We have collected and reared from hatching boreal copepods in the laboratory (*Calanus finmarchicus*). These animals have been exposed to radionuclides in radiolabeled phytoplankton food and the assimilation of ingested radionuclides has been measured. The results at two different

temperatures (to assess the uniqueness of polar conditions on the trophic transfer of radionuclides) were compared. This copepod species was also compared with results from temperate copepod species (calanoid copepods *Acartia tonsa*, *Acartia hudsonica*, and *Temora longicornis*) collected from Long Island Sound.

E. Results

Table 1 summarizes the assimilation efficiencies determined for Am-241, Co-57, Fe-59, and Eu-152. Note that Cs-137 was not accumulated from the dissolved phase by the diatoms (phytoplankton food used in these experiments), and so it was impossible to determine the assimilation of ingested Cs in these zooplankton. These results suggest that the trophic transfer of Cs at the lower end of the food chain is unlikely to be important in marine systems. Assimilation efficiencies ranged from 1% for Am and Eu to 12% for Co at 2 C. Assimilation efficiencies of these radionuclides at 12 C were also lowest for Am and Eu and highest for Co. A repeat of this experiment, using a different batch of *C. finmarchicus*, yielded approximately similar results (Table 1). We concluded from these experiments that of the radioisotopes examined, only Co has non-negligible assimilation from phytoplankton food in marine copepods. Table 1 also shows the results from two separate experiments, also with different batches of freshly collected copepods, that temperate species (*Acartia* spp. and *T. longicornis*) responded to these ingested radionuclides very similarly to the polar copepods.

We also measured the depuration rates of these radionuclides from the copepods, to determine the extent to which these elements are retained by the copepods over time. Depuration rate constants (in units of day⁻¹) and biological half-lives ($tb_{1/2}$) of the radioisotopes in the copepods are given in Table 2. Results indicate that for *C. finmarchicus* isotopes were lost at comparable rates at 2 C and 12 C from the animals, with the possible exception of Eu-152 (Table 2). Biological half-lives were on the order of 20-40 days in the polar copepods. For comparison purposes, depuration rate constants and biological half-lives are also given for these radionuclides in the temperate copepod species (Table 2).

Figs. 1-4 present the distribution of the radioisotopes among *C. finmarchicus* copepods, copepod fecal pellets, the dissolved phase, and phytoplankton prey cells at 2 and 12 C. Note that for the most particle-reactive metals (Am, Fe, and Eu), there is very little radionuclide remaining in the copepods after gut evacuation (reflecting the very low assimilation efficiencies) but rather high amounts in the copepod fecal matter. These fecal pellets, which sink at rates ≥ 100 m d⁻¹, could serve to vertically transport these radionuclides to deep waters and sediments. Figs. 5-8 show the results from the second trial with another batch of *C. finmarchicus*. The results are strikingly similar to the first set of experiments. For comparison purposes, the results of comparable experiments using *Acartia* spp. and *T. longicornis* are presented in Figs. 9-12. Again, similar conclusions could be drawn for these temperate species copepods.

F. Impact for science or systems applications

These data are relevant to understanding the uptake and cycling of long-lived radionuclides released into the Kara Sea in marine plankton communities there. Further, the results indicate that

the processes operating at polar temperatures (2 C) do not yield profoundly different results for the trophic transfer of these radionuclides than do the same processes at warmer temperatures.

G. Transitions expected

None.

H. Relationship to other projects

I have been funded to work on the fate of radionuclides transported in the Ob River. I have also been funded to examine the use of benthic invertebrates in the Kara Sea as potential bioindicator organisms of released radionuclides. Many of the same processes operating on the trophic transfer of radionuclides as studied in this project are relevant to those other studies.

I. Application to the Arctic radioactive waste assessment problem

These results will be used to help the risk assessment activities of the ANWAP program. Specifically, the risks associated with consumption of seafood deriving from Arctic waters requires input on bioconcentration factors for long-lived radionuclides in important components of the marine food web. It also requires input on how organisms can mediate the cycling and vertical flux of these radionuclides in marine systems. Copepods and other zooplankton can, through their debris, profoundly influence these fluxes and thereby affect the residence times of these radionuclides in Arctic water columns.

II. Statistical Information

A. List of publications

Hutchins, D.A., W.-X. Wang, and N.S. Fisher. 1995. Copepod grazing and the biogeochemical fate of diatom iron. *Limnology and Oceanography* 40: 989-994.

Wang, W.-X., J.R. Reinfelder, B.-G. Lee, and N.S. Fisher. 1996. Assimilation and regeneration of trace elements by marine copepods. *Limnology and Oceanography* 41: 70-81.

Wang, W.-X., and N.S. Fisher. in press. Accumulation of trace elements in a marine copepod. *Limnology and Oceanography*.

Wang, W.-X., and N.S. Fisher. submitted. Excretion of trace elements in marine copepods and their bioavailability to diatoms. *Journal of Marine Research*.

Hutchins, D.A., W.-X. Wang, M. Schmidt, and N.S. Fisher. submitted. Double-labeling techniques for trace metal biogeochemical investigations in marine and freshwater plankton communities. *Limnology and Oceanography*.

Fisher, N.S., S.W. Fowler, F. Boisson, J.L. Carroll, K. Rissanen, B. Salbu, T.G. Sazykina, and K.L. Sjoebom. submitted. Bioconcentration factors and sediment partition coefficients for radionuclides in contaminated Arctic seas. *Environmental Science and Technology*/

B. Number of graduate students

Two grad students: Sharon Hook, Christopher Hoimes. Two postdocs: David Hutchins, Christian Gagnon.

C. Patents

None.

D. Presentations

None.

E. Committed Service

None.

F. Awards

None.

G. Russian participation

None.

Fig. 1. Distribution of Am-241 among *Calanus finmarchicus* copepods, copepod fecal pellets, dissolved phase (< 0.2 μ m), and phytoplankton prey cells following 24 hours of depuration from the copepods. Data are for 2 and 12 C experiments, trial 1; all experiments run with three replicate microcosms, each with hundreds of copepods.

Fig. 2. Distribution of Co-57 among *Calanus finmarchicus* copepods, copepod fecal pellets, dissolved phase (< 0.2 μ m), and phytoplankton prey cells following 24 hours of depuration from the copepods. Data are for 2 and 12 C experiments, trial 1; all experiments run with three replicate microcosms, each with hundreds of copepods.

Fig. 3. Distribution of Fe-59 among *Calanus finmarchicus* copepods, copepod fecal pellets, dissolved phase (< 0.2 μ m), and phytoplankton prey cells following 24 hours of depuration from the copepods. Data are for 2 and 12 C experiments, trial 1; all experiments run with three replicate microcosms, each with hundreds of copepods.

Fig. 4. Distribution of Eu-152 among *Calanus finmarchicus* copepods, copepod fecal pellets, dissolved phase (< 0.2 μ m), and phytoplankton prey cells following 24 hours of depuration from the copepods. Data are for 2 and 12 C experiments, trial 1; all experiments run with three replicate microcosms, each with hundreds of copepods.

Fig. 5. Distribution of Am-241 among *Calanus finmarchicus* copepods, copepod fecal pellets, dissolved phase (< 0.2 μ m), and phytoplankton prey cells following 24 hours of depuration from the copepods. Data are for 2 and 12 C experiments, trial 2; all experiments run with three replicate microcosms, each with hundreds of copepods.

Fig. 6. Distribution of Co-57 among *Calanus finmarchicus* copepods, copepod fecal pellets, dissolved phase (< 0.2 μ m), and phytoplankton prey cells following 24 hours of depuration from the copepods. Data are for 2 and 12 C experiments, trial 2; all experiments run with three replicate microcosms, each with hundreds of copepods.

Fig. 7. Distribution of Fe-59 among *Calanus finmarchicus* copepods, copepod fecal pellets, dissolved phase (< 0.2 μ m), and phytoplankton prey cells following 24 hours of depuration from the copepods. Data are for 2 and 12 C experiments, trial 2; all experiments run with three replicate microcosms, each with hundreds of copepods.

Fig. 8. Distribution of Eu-152 among *Calanus finmarchicus* copepods, copepod fecal pellets, dissolved phase (< 0.2 μ m), and phytoplankton prey cells following 24 hours of depuration from the copepods. Data are for 2 and 12 C experiments, trial 2; all experiments run with three replicate microcosms, each with hundreds of copepods.

Fig. 9. Distribution of Am-241 among *Acartia* spp. and *Temora longicornis* copepods, copepod fecal pellets, dissolved phase (< 0.2 μ m), and phytoplankton prey cells following 24 hours of depuration from the copepods. Data are for 6 and 16 C experiments; all experiments run with three replicate microcosms, each with hundreds of copepods.

Fig. 10. Distribution of Co-57 among *Acartia* spp. and *Temora longicornis* copepods, copepod fecal pellets, dissolved phase ($< 0.2 \mu\text{m}$), and phytoplankton prey cells following 24 hours of depuration from the copepods. Data are for 6 and 16 C experiments; all experiments run with three replicate microcosms, each with hundreds of copepods.

Fig. 11. Distribution of Fe-59 among *Acartia* spp. and *Temora longicornis* copepods, copepod fecal pellets, dissolved phase ($< 0.2 \mu\text{m}$), and phytoplankton prey cells following 24 hours of depuration from the copepods. Data are for 6 and 16 C experiments; all experiments run with three replicate microcosms, each with hundreds of copepods.

Fig. 12. Distribution of Eu-152 among *Acartia* spp. and *Temora longicornis* copepods, copepod fecal pellets, dissolved phase ($< 0.2 \mu\text{m}$), and phytoplankton prey cells following 24 hours of depuration from the copepods. Data are for 6 and 16 C experiments; all experiments run with three replicate microcosms, each with hundreds of copepods.

Summary of Assimilation Efficiencies of Radionuclides in Copepods

***Calanus finmarchicus* Trial 1**

Isotope	12°C	2°C
Am-241	0.02 +/- 0.03	0.01 +/- 0.01
Co-57	0.05 +/- 0.02	0.12 +/- 0.01
Fe-59	0.03 +/- 0.02	0.03 +/- 0.01
Eu-152	0.02 +/- 0.02	0.01 +/- 0.00

***Calanus finmarchicus* Trial 2**

Isotope	12°C	2°C
Am-241	0.02 +/- 0.02	0.03 +/- 0.01
Co-57	0.06 +/- 0.01	0.10 +/- 0.01
Fe-59	0.02 +/- 0.02	0.03 +/- 0.01
Eu-152	0.01 +/- 0.00	0.05 +/- 0.03

***Acartia* sp. and *Temora longicornis* Trial 1**

Isotope	16°C	6°C
Am-241	0.01 +/- 0.00	0.06 +/- 0.07
Co-57	0.05 +/- 0.00	0.09 +/- 0.03
Fe-59	0.02 +/- 0.01	0.00 +/- 0.00
Eu-152	0.01 +/- 0.00	0.01 +/- 0.01

***Acartia* sp. and *Temora longicornis* Trial 2**

Isotope	16°C	6°C
Am-241	0.03 +/- 0.03	0.02 +/- 0.02
Co-57	0.09 +/- 0.01	0.12 +/- 0.05
Fe-59	0.21 +/- 0.05	0.07 +/- 0.06
Eu-152	0.15 +/- 0.14	0.01 +/- 0.01

TABLE 1.

Depuration Rate of Radionuclides in Copepods

Calanus finmarchicus Trial 1

Isotope	12°C	tb _{1/2} (d)	2°C	tb _{1/2} (d)
Am-241	.022	31.5	.028	24.8
Co-57	.021	33.0	.019	36.5
Fe-59	.020	34.65	.021	33.0
Eu-152	.014	49.5	.030	23.1

Calanus finmarchicus Trial 2

Isotope	12°C	tb _{1/2} (d)	2°C	tb _{1/2} (d)
Am-241	.025	27.7	.019	36.5
Co-57	.023	30.1	.019	36.5
Fe-59	.034	20.4	.025	27.7
Eu-152	.011	63.0	.009	77.0

Acartia sp. and *Temora longicornis* Trial 1

Isotope	16°C	tb _{1/2} (d)	6°C	tb _{1/2} (d)
Am-241	.011	63.0	.001	693
Co-57	.016	43.3	.011	63.0
Fe-59	.008	86.6		
Eu-152	.010	69.3	.003	231

Acartia sp. and *Temora longicornis* Trial 2

Isotope	16°C	tb _{1/2} (d)	6°C	tb _{1/2} (d)
Am-241	.016	43.3	.008	86.6
Co-57	.020	34.7	.013	53.3
Fe-59	.017	40.8	.011	63.0
Eu-152	.004	173.3	.006	116

TABLE 2.

Fig. 1. Distribution of Am-241 among *Calanus finmarchicus* copepods, copepod fecal pellets, dissolved phase (< 0.2 μm), and phytoplankton prey cells following 24 hours of depuration from the copepods. Data are for 2 and 12 C experiments, trial 1; all experiments run with three replicate microcosms, each with hundreds of copepods.

Fig. 2. Distribution of Co-57 among *Calanus finmarchicus* copepods, copepod fecal pellets, dissolved phase (< 0.2 μm), and phytoplankton prey cells following 24 hours of depuration from the copepods. Data are for 2 and 12 C experiments, trial 1; all experiments run with three replicate microcosms, each with hundreds of copepods.

Fig. 3. Distribution of Fe-59 among *Calanus finmarchicus* copepods, copepod fecal pellets, dissolved phase (< 0.2 μm), and phytoplankton prey cells following 24 hours of depuration from the copepods. Data are for 2 and 12 C experiments, trial 1; all experiments run with three replicate microcosms, each with hundreds of copepods.

Fig. 4. Distribution of Eu-152 among *Calanus finmarchicus* copepods, copepod fecal pellets, dissolved phase (< 0.2 μm), and phytoplankton prey cells following 24 hours of depuration from the copepods. Data are for 2 and 12 C experiments, trial 1; all experiments run with three replicate microcosms, each with hundreds of copepods.

Fig. 5. Distribution of Am-241 among *Calanus finmarchicus* copepods, copepod fecal pellets, dissolved phase (< 0.2 μm), and phytoplankton prey cells following 24 hours of depuration from the copepods. Data are for 2 and 12 C experiments, trial 2; all experiments run with three replicate microcosms, each with hundreds of copepods.

Fig. 6. Distribution of Co-57 among *Calanus finmarchicus* copepods, copepod fecal pellets, dissolved phase (< 0.2 μm), and phytoplankton prey cells following 24 hours of depuration from the copepods. Data are for 2 and 12 C experiments, trial 2; all experiments run with three replicate microcosms, each with hundreds of copepods.

Fig. 7. Distribution of Fe-59 among *Calanus finmarchicus* copepods, copepod fecal pellets, dissolved phase (< 0.2 μm), and phytoplankton prey cells following 24 hours of depuration from the copepods. Data are for 2 and 12 C experiments, trial 2; all experiments run with three replicate microcosms, each with hundreds of copepods.

Fig. 8. Distribution of Eu-152 among *Calanus finmarchicus* copepods, copepod fecal pellets, dissolved phase (< 0.2 μm), and phytoplankton prey cells following 24 hours of depuration from the copepods. Data are for 2 and 12 C experiments, trial 2; all experiments run with three replicate microcosms, each with hundreds of copepods.

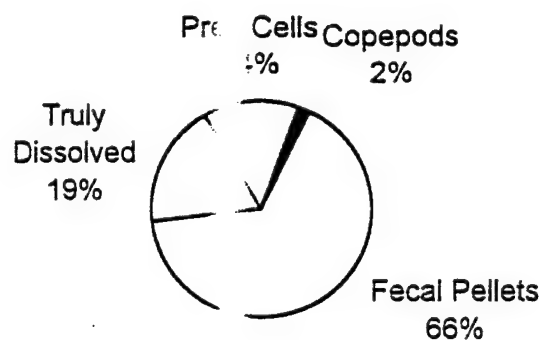
Fig. 9. Distribution of Am-241 among *Acartia* spp. and *Temora longicornis* copepods, copepod fecal pellets, dissolved phase (< 0.2 μm), and phytoplankton prey cells following 24 hours of depuration from the copepods. Data are for 6 and 16 C experiments; all experiments run with three replicate microcosms, each with hundreds of copepods.

Fig. 10. Distribution of Co-57 among *Acartia* spp. and *Temora longicornis* copepods, copepod fecal pellets, dissolved phase ($< 0.2 \mu\text{m}$), and phytoplankton prey cells following 24 hours of depuration from the copepods. Data are for 6 and 16 C experiments; all experiments run with three replicate microcosms, each with hundreds of copepods.

Fig. 11. Distribution of Fe-59 among *Acartia* spp. and *Temora longicornis* copepods, copepod fecal pellets, dissolved phase ($< 0.2 \mu\text{m}$), and phytoplankton prey cells following 24 hours of depuration from the copepods. Data are for 6 and 16 C experiments; all experiments run with three replicate microcosms, each with hundreds of copepods.

Fig. 12. Distribution of Eu-152 among *Acartia* spp. and *Temora longicornis* copepods, copepod fecal pellets, dissolved phase ($< 0.2 \mu\text{m}$), and phytoplankton prey cells following 24 hours of depuration from the copepods. Data are for 6 and 16 C experiments; all experiments run with three replicate microcosms, each with hundreds of copepods.

Ar 12C



Ar 2C

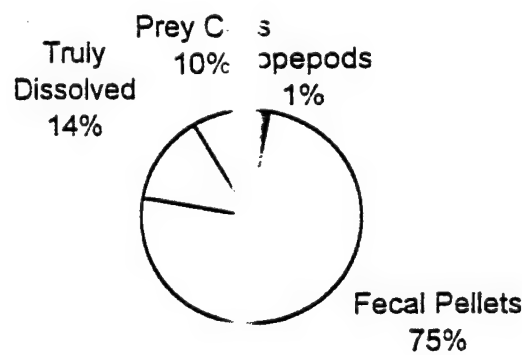
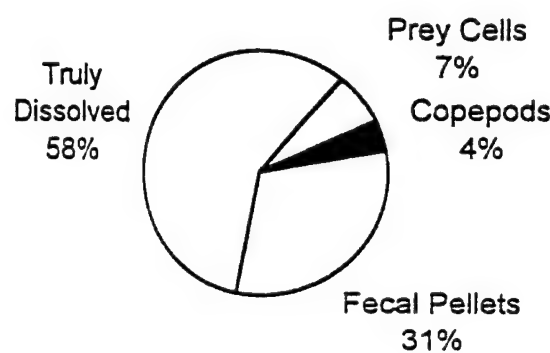


Figure 1.

Co 12C



Co 2C

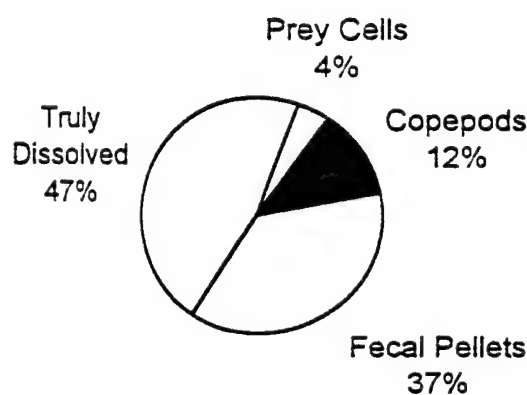
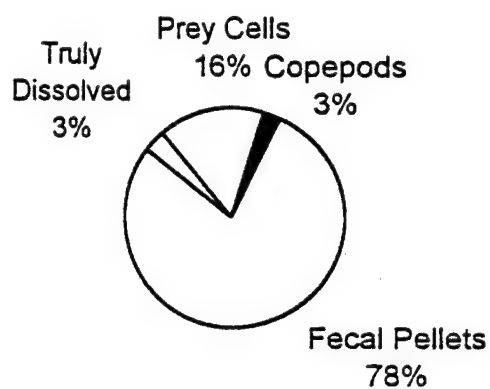


Figure 2.

Fe 12C



Fe 2C

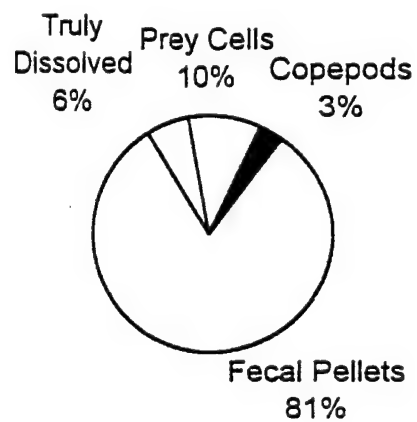


Figure 3.

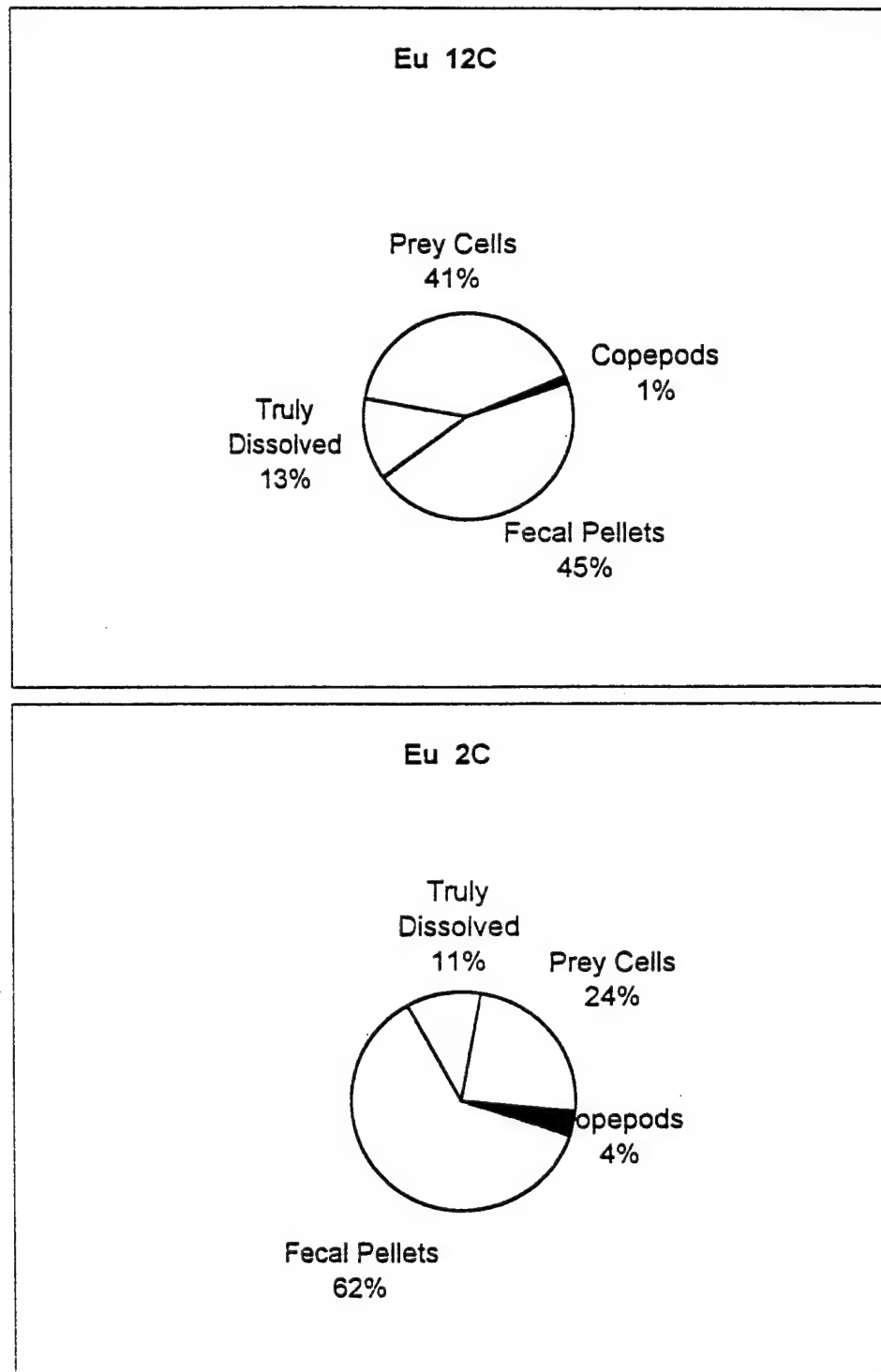
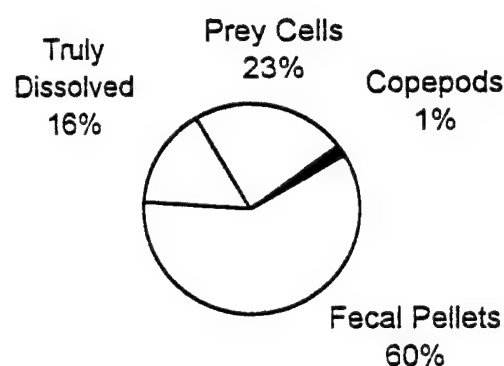


Figure 4.

Am 12C



Am 2C

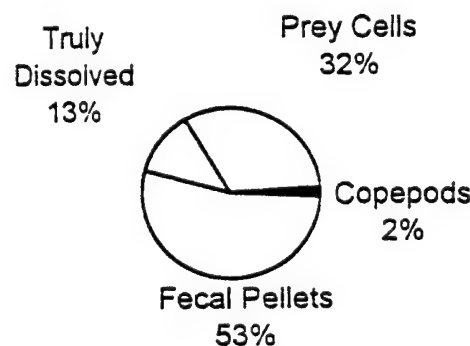
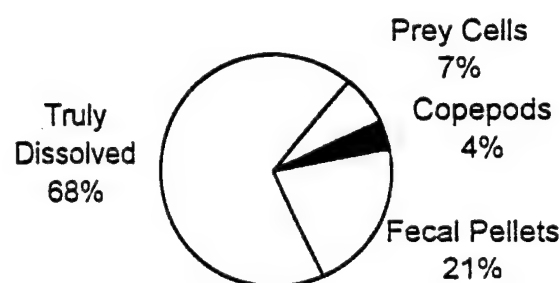


Figure 5.

Co 12C



Co 2C

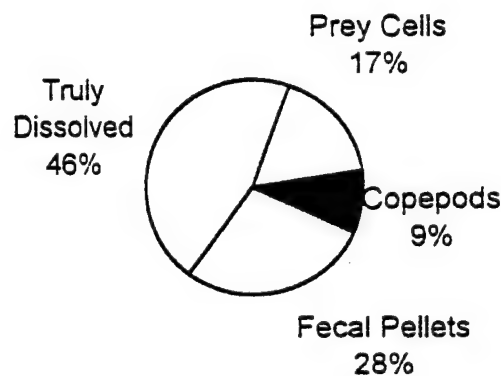
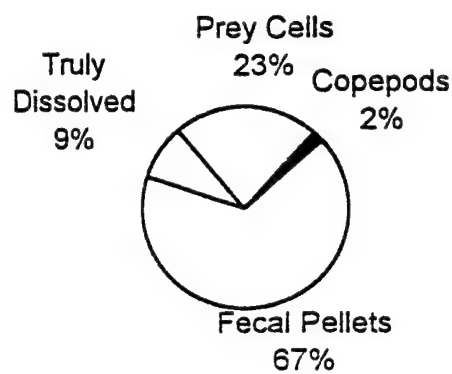


Figure 6.

Fe 12C



Fe 2C

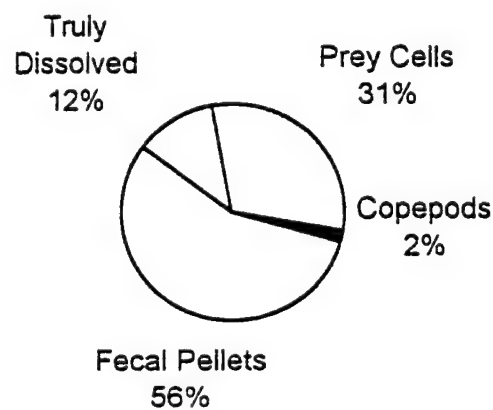
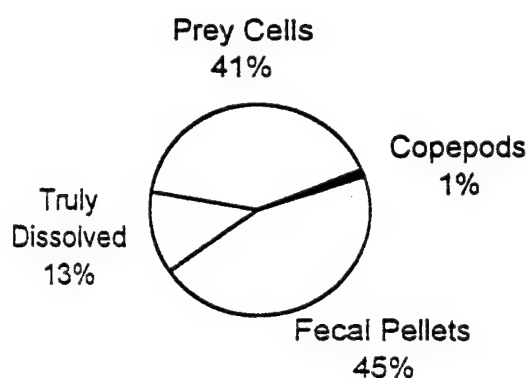


Figure 7.

Eu 12C



Eu 2C

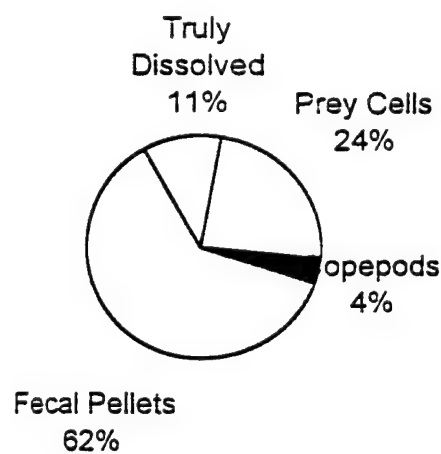


Figure 8.

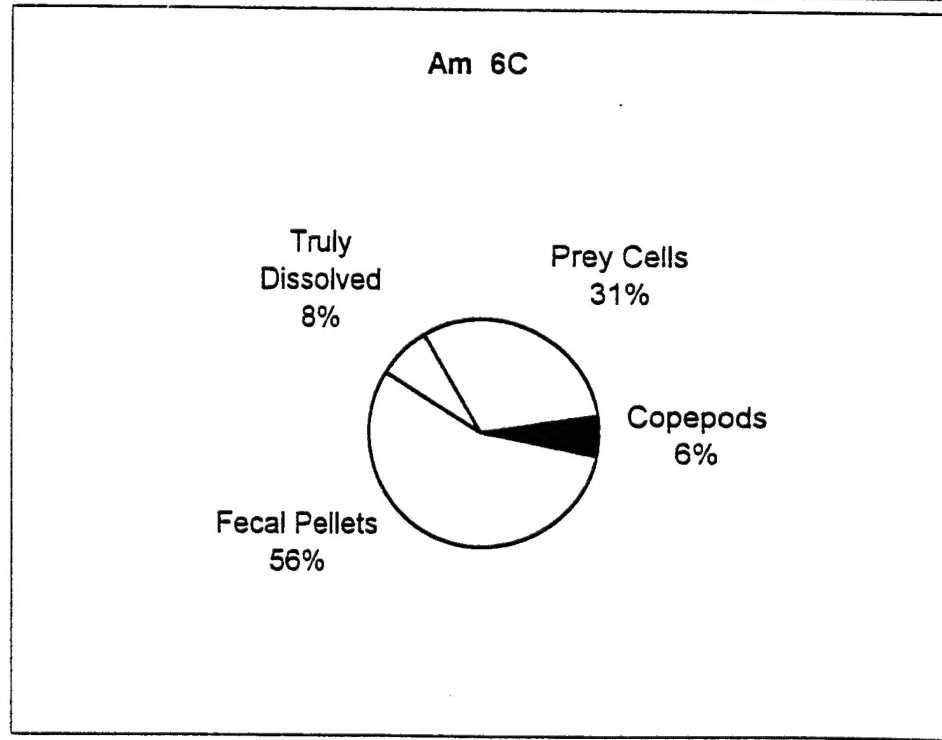
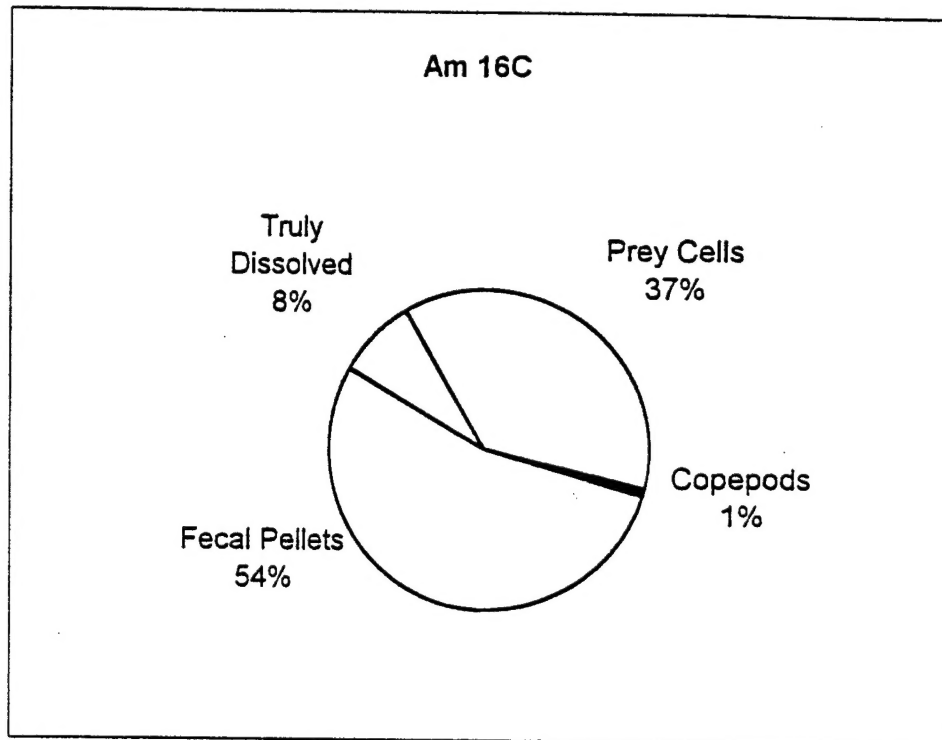
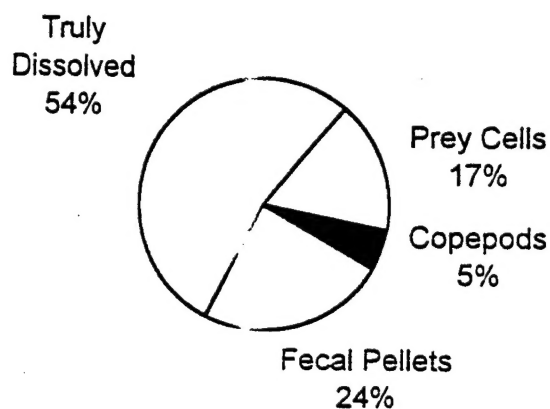


Figure 9.

Co 16C



Co 3C

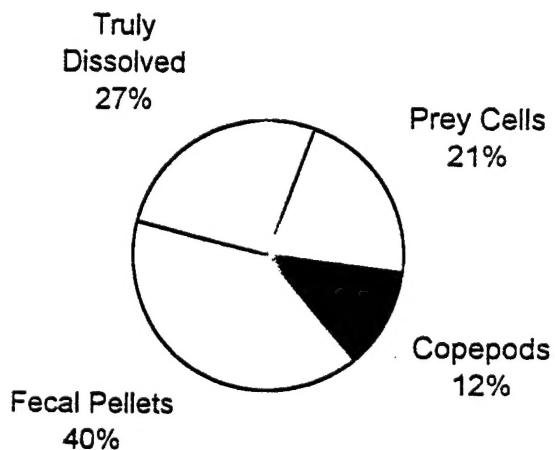
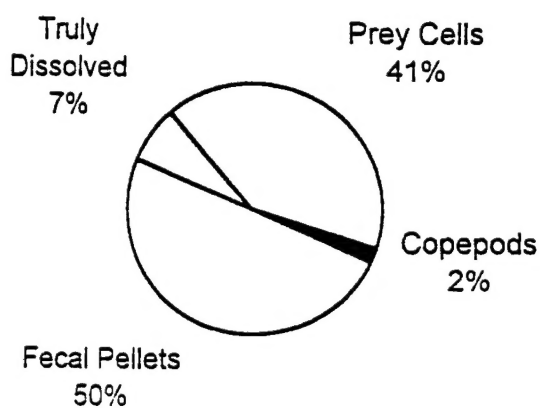


Figure 10.

Fe 16C



Fe 6C

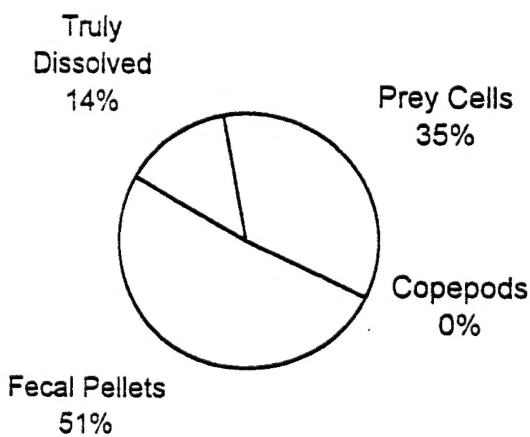
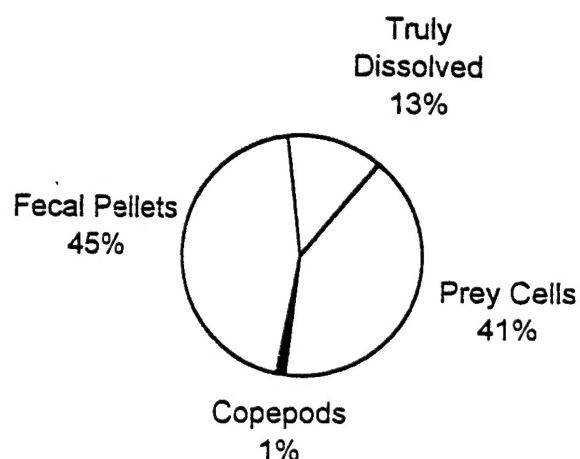


Figure 11.

Eu 16C



Eu 6C

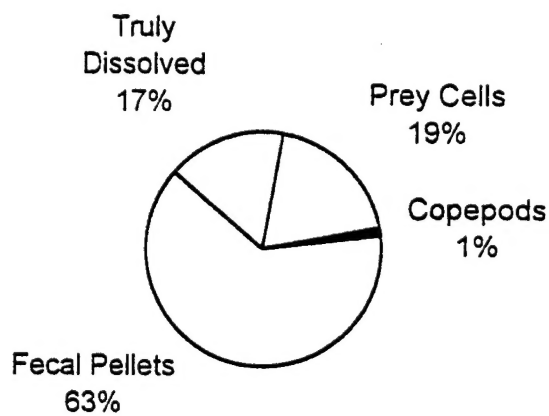


Figure 12.